COMPARISON OF RAY-THEORY SYNTHETIC SEISMOGRAMS WITH FINITE-DIFFERENCES IN 2D VELOCITY MODEL UNCONFORMITY

LUDEK KLIMEŠ

Department of Geophysics, Faculty of Mathematics and Physics, Charles University, Ke Karlovu 3, 12116 Prague 2, Czech Republic.

(Received November 6, 2020; accepted January 4, 2121)

ABSTRACT

Klimeš, L., 2021. Comparison of ray-theory synthetic seismograms with finite-differences in 2D velocity model UNCONFORMITY. *Journal of Seismic Exploration*, 30: 271-279.

Synthetic seismograms for an explosive point source in 2D elastic velocity model UNCONFORMITY are calculated by a 3D ray method and by 2D finite-differences followed by an approximate conversion from a line source to a point source. The demonstrated differences between 3D ray-theory seismograms and converted 2D finite-difference seismograms are discussed in detail.

KEY WORDS: velocity model, elastic waves, synthetic seismograms, ray-theory, finite-differences.

INTRODUCTION

We wish to compare the ray-theory synthetic seismograms with the finite-difference synthetic seismograms in order to observe the inaccuracy of the ray-theory. Since we have a 2D finite-difference code only, we have to consider a 2D velocity model. We choose 2D elastic velocity model UNCONFORMITY by Cormier and Mellen (1984), whereas the previous comparison was performed in a very simple 1D elastic velocity model (Klimeš, 2019). The synthetic seismograms in velocity model UNCONFORMITY were already calculated by Cormier and Mellen (1984) using ray-theory and by Musil (1989) using Gaussian beam summation. Klimeš (2020) then demonstrated the effect of attenuation in the viscoelastic version of velocity model UNCONFORMITY.

We consider 3D synthetic seismograms for a point source. While 3D calculations represent no problem for ray methods, we have to approximately convert 2D finite-difference seismograms calculated for a line source into seismograms corresponding to a point source. We apply the approximate conversion described by Klimeš (2019, eqs. 5, 6).

0963-0651/21/$5.00

In this paper, we compare the 3D ray-theory seismograms with 2D finite-difference seismograms in 2D elastic velocity model UNCONFORMITY, and discuss the differences between the seismograms in detail.

For the ray-theory and finite-difference computer codes and for the data corresponding to the presented example refer to Bucha and Bulant (2019). For the step-by-step explanation of the data refer to Bucha and Klimeš (1999).

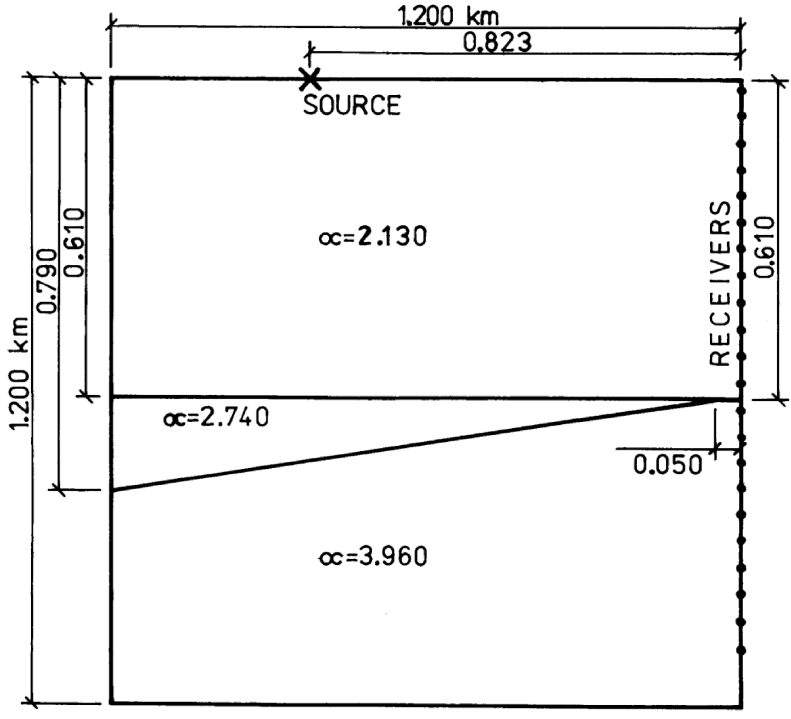

Fig. 1. Two–dimensional velocity model UNCONFORMITY by Cormier and Mellen (1984) composed of 3 homogeneous blocks. P-wave velocities are denoted by α .

VELOCITY MODEL UNCONFORMITY, SOURCE AND RECEIVERS

Two–dimensional velocity model UNCONFORMITY by Cormier and Mellen (1984), situated in a vertical square 1.2 km x 1.2 km, is composed of three homogeneous blocks separated by planar interfaces and forming a simplified pinchout. The geometry of the velocity model, P-wave velocities α and the positions of the point source and of 22 receivers are depicted in Fig. 1. The origin of the Cartesian coordinate system is selected in the left top corner, with horizontal axis x_1 pointing to the right and vertical axis x_3 pointing upwards.

For the P-wave velocities α in three homogeneous blocks refer to Fig.1. The S-wave velocities are specified by relation

$$\beta = 0.57735\ \alpha \quad . \tag{1}$$

The densities in all 3 blocks are given by

$$\partial/\mathrm{g\ cm^{-3}} = 1.7 + 0.2(\alpha/\mathrm{km\ s^{-1}}) \quad . \tag{2}$$

We consider the unit seismic moment of an explosive source, because the used finite-difference program considers the explosive source only. The rotation centre used by Klimeš (2020) cannot be considered.

Instead of the Gabor signal used by Klimeš (2020), we have to apply the Küpper signal (Küpper, 1958; Müller, 1970) with 2 local maxima because the used finite-difference program does not support another source time function. The reference frequency of 100 Hz used by Klimeš (2020) is decreased to 10 Hz because of finite-differences, as discussed in a next Section. The line source in the 2D finite-difference program is excited by the Küpper signal at 3 x 3 gridpoints.

We calculate the 3D synthetic seismograms from an explosive point source using the 3D ray method. However, we use 2D finite differences for comparison, because we have no 3D finite–difference code. The finite-difference seismograms thus correspond to a line source. We wish to approximate the point source by the line source excited by the Küpper signal in the 2D finite-difference program. We thus take the half-th derivative of the Küpper signal as the source time function describing the time dependence of the seismic moment of the explosive point source (Klimeš, 2019, eq. 5). Then the point and line sources generate wavelets of the same form in the far-field approximation.

The seismograms are plotted between times 0.300 s and 1.000 s. The amplitude scale corresponds to a point source in 3D.

To be able to plot also the 2D finite-difference seismograms, corresponding to the line source, in a comparable scale, we choose the reference distance for the amplitude power scaling during the plotting equal to the hypocentral distance (in a homogeneous medium), at which the wave fields generated by the point and line sources have the same amplitudes (Klimeš, 2019, eq. 7).

When plotting, we will use no amplitude power scaling for the point source but the power scaling, proportional to the hypocentral distance powered to $-1/2$, for the line source. In this way, seismograms corresponding to the point and line sources will coincide in the neighbourhood of the source point. They, of course, may considerably differ for reflected waves and at large distances in a heterogeneous medium.

RAY-THEORY SYNTHETIC SEISMOGRAMS

The selection of 9 elementary waves for ray tracing from the explosive point source is performed according to Cormier and Mellen (1984, Table 2-3, Figs. 2-12, 2-13).

Application of programs to calculate ray-theory synthetic seismograms is conditioned by reasonably reliable two-point ray tracing. Each missing two-point ray creates a gap in the synthetic seismograms and each erroneously doubled two-point ray doubles the amplitude of the corresponding arrival. Bulant (1996, 1999) supplemented our ray-tracing code (Červený et al., 1988; Bucha and Bulant, 2019) with 3D two-point ray-tracing by the shooting method, which enables us to calculate ray-theory synthetic seismograms in 3D heterogeneous velocity models. The ray-theory synthetic seismograms are calculated in the frequency domain and converted to the time domain using the Fast Fourier Transform (Červený, 2001).

We apply the cosine window specified by frequencies 0 Hz, 1 Hz, 55Hz and 60 Hz to filter the source time function in order to remove low or negative frequencies for the ray method. Since finite-difference program does not filter the signal, the filtering should not distort the signal. The time step of 0.001 s and the time interval of 1.023 s are specified for the Fast Fourier Transform. However, the time step could be chosen considerably longer in this case.

FINITE–DIFFERENCE SYNTHETIC SEISMOGRAMS

Finite–difference software package

The basis of the finite-difference package is the code for 2D P-SV elastic second-order finite-differences written by Jiˇrí Zahradník (Zahradník 1995; Zahradník and Priolo, 1995). The code, however, utilizes a specific technique to build the velocity models of geological structures. The technique is not compatible with the velocity models specified for the ray methods (Červený, 1988).

In a vicinity of interfaces, the finite–difference code applies the "effective" elastic parameters at the gridpoints of the finite–difference grid. For the description of "effective" elastic parameters refer to Bucha and Klimeš (1999).

The Fortran code for 2D P-SV elastic second-order finite-differences has thus been split into two parts: program generating gridded "effective" elastic parameters and the finite-difference program. The modified finite-difference code can read the velocity model specified for the ray methods.

Calculating finite–difference synthetic seismograms

Finite-differences are often limited by the memory requirements or by the computational costs. This is also the case of the grid dimensions in our example.

In the first finite-difference calculation, we wish to locate the finite-difference code within 16 MB of available RAM.

The top boundary of the finite-difference grid is a free earth surface in the finite-difference program. Since we consider no free surface in the ray-theory calculations and wish to have the same velocity model, the reflections from the top of the grid should arrive at the uppermost receiver, situated 0.017 km below the source, at the least, after the P-wave reflected from the horizontal interface 0.610 km below the source. We thus wish the top of the grid higher than $d'_3 = 0.610$ km − 0.017 km = 0.593 km above the source. The horizontal source-receiver distance is $d_1 = 0.823$ km and the lowermost receiver is situated $d''_3 = 1.088$ km below the source. The grid thus should cover region d_1 times $d_3 = d'_3 + d''_3 = 1.681$ km. For grid interval D, it requires $N_1 = d_1/(D+41)$ times $N_3 = d_3/(D+21)$ gridpoints, where 20 gridpoints are reserved for the dumpers at the left-hand, bottom and right–hand grid margins. The grid interval then has to be longer than 0.0026 km in order to fit the available RAM. We thus choose grid interval $D = 0.003$ km for the finite-differences, with horizontal and vertical grid dimensions $N_1 = 316$ and $N_3 = 646$, respectively. The grid covers the rectangle extending horizontally from 0.315 km to 1.260 km, and vertically from −1.149 km to 0.786 km. The grid begins horizontally 0.062 km to the left from the source and ends 0.060 km to the right from the receivers. The top of the grid is located 0.786 km above the source, and the bottom of the grid is located 0.061 km below the lowermost receiver.

The time step must satisfy stability condition

$$D_t < D/(1.65\, v_{max}) \quad , \tag{3}$$

where v_{max} is the maximum P-wave velocity in the velocity model, here $v_{max} = 3.960$ km s^{-1}, which results in $D_t < 0.000459$ s. We choose $D_t = 0.0004$ s. The number of time levels from 0 s to 1 s is then $N_t = 2501$.

The relative wave-field error due to the grid dispersion of the second-order finite-differences, accumulated along distance s in a homogeneous medium with $v^2_P \leq 3v^2_S$, is (Klimeš, 1996, eqs. 24, 33, 108, 110)

$$\Delta_u \approx (2\pi f / v)^3 (D^2 s / 24) \quad . \tag{4}$$

The considerable part of the error is accumulated by the S-wave travelling from the interface 0.610 km below the source to the uppermost receiver. The distance is about $s \approx 0.6$ km and the velocity is 2.13 km s$^{-1}/\sqrt{3}$. Then the relative error of the harmonic S-wave is roughly

$$\Delta_u \approx (f\ 0.03\ s)^3 \quad . \tag{5}$$

It is obvious that we cannot use 100 Hz source time function as Klimeš (2020) did for the ray method. Choosing the Küpper signal of reference frequency at 10 Hz, we probably keep the relative error below something like 4%.

Since the "nonreflecting" boundary conditions of finite-differences may, to some extent, reflect the waves, it is highly recommended to change the finite-difference grid roughly by a quarter of the prevailing wavelength and to run the finite-differences once again. The reflections from the boundaries are then shifted roughly by half the prevailing period and are clearly visible in the common plots of the seismograms from both the computations. Moreover, in this example we have also very strong unwanted reflections from the free surface at the top of the finite-difference grid.

The reference P-wave wavelength is 71 to 132 grid intervals, the S-wave wavelength is 41 to 76 grid intervals. We thus enlarge the grid by 20 grid intervals at all 4 sides in the second finite-difference calculation.

COMPARISON OF THE SYNTHETIC SEISMOGRAMS

We plot the calculated synthetic seismograms together, in the colour PostScript plots of the horizontal in-plane and vertical components. The transversal component is zero.

The calculated seismograms are shown in Figs. 2 and 3, where the reflections from the nonreflecting boundaries can clearly be identified. The blue reflections (the first finite-difference calculation) come before the green ones (the second finite-difference calculation with the enlarged grid). The 2D finite-difference seismograms are overlaid by the red 3D ray-theory synthetic seismograms.

Where blue and green seismograms coincide, the finite-difference seismograms are not distorted by reflections from the non-reflecting boundaries.

The most pronounced drawbacks of the ray-theory are highlighted in pastel colours. From the left, the ghost green indicates the increased ray-theory amplitudes in the vicinity of the P-wave critical angle, which is somewhere around the second receiver from the left. The light yellow colour indicates the gap in the reflected P-S wave due to the missing diffracted wave which should fill the ray-theory shadow zone between reflections from the two interfaces. The light orange (sand) indicates the distorted amplitudes just below the interface at the depth of 0.610 km due to the missing first-order ray-theory approximations of refracted waves.

Except for the above mentioned problems, the finite-difference and ray-theory seismograms are in a good agreement, especially if we consider the difference between the point and line sources.

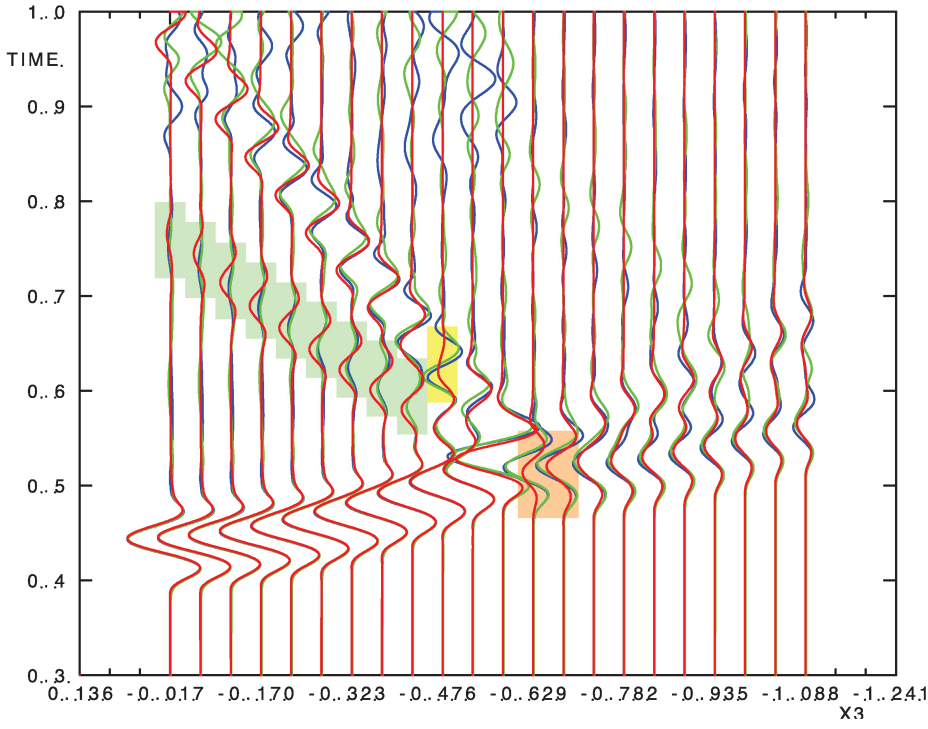

Fig. 2. Horizontal component of the synthetic seismograms in the UNCONFORMITY velocity model. 2D finite-differences are blue and green, 3D ray method is red. For a more detailed description refer to the text.

The inaccuracy of ray-theory in this velocity model is considerably smaller than the effect of possible attenuation (Klimeš, 2020).

CONCLUSIONS

Ray methods are not accurate, especially in a vicinity of structural interfaces. This is a well-known property of ray methods.

On the other hand, ray methods have some advantages in comparison with finite-differences. Finite-differences are usually coded for elastic media and their extension to viscoelastic media is difficult, while

attenuation is present all over the Earth and cannot be neglected in numerical modelling of seismic wave propagation. Finite-differences are often limited by the memory requirements or by the computational costs, which results in a small maximum frequency of the wave field, especially in 3D. Another problem is that the absorbing boundary conditions and dumpers for finite-differences often do not work perfectly. The reflections from the boundaries may be identified in seismograms by calculating the seismograms with two different positions of the boundaries and comparing the results, see, e.g., Figs. 2 and 3 of this paper or Klimeš (2019).

The presented example demonstrate the inaccuracy of the ray-theory in a vicinity of structural interfaces. The inaccuracy of the ray-theory in this velocity model is considerably smaller than the effect of possible attenuation (Klimeš, 2020).

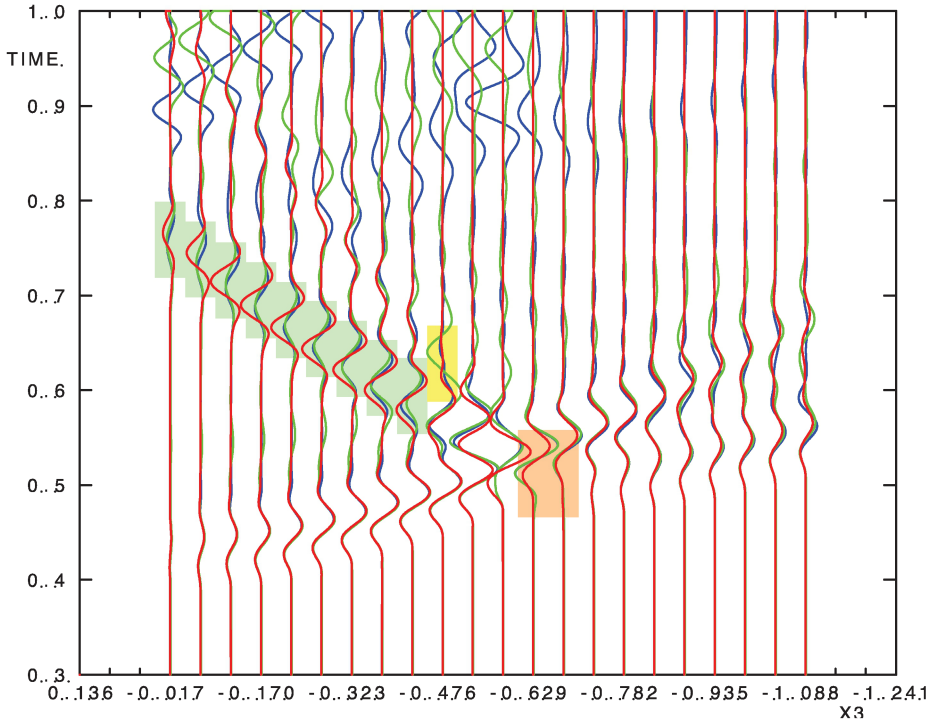

Fig. 3. Vertical component of the synthetic seismograms in the UNCONFORMITY velocity model. 2D finite-differences are blue and green, 3D ray method is red. For a more detailed description refer to the text.

ACKNOWLEDGEMENTS

I am indebted to Jirí Zahradník, the author of the finite-difference code, for his kind and patient assistance in preparing the finite-difference package used in this paper.

The research has been supported by the Czech Science Foundation under contract 20-06887S, and by the members of the consortium "Seismic Waves in Complex 3-D Structures" (see "http://sw3d.cz").

REFERENCES

Bucha, V. and Bulant, P. (Eds.), 2019. SW3D-CD-23 (DVD-ROM). Seismic Waves in Complex 3-D Structures, 29: 71-72. http://sw3d.cz.

Bucha, V. and Klimeš, L., 1999. Finite-differences above the MODEL package. Seismic Waves in Complex 3-D Structures, 8: 171-192. http://sw3d.cz.

Bulant, P., 1996. Two-point ray-tracing in 3-D. Pure Appl. Geophys., 148: 421-447.

Bulant, P., 1999. Two-point ray-tracing and controlled initial-value ray-tracing in 3-D heterogeneous block structures. J. Seismic Explor., 8: 57-75.

Červený, V., 2001. Seismic Ray Theory. Cambridge University Press, Cambridge.

Červený, V., Klimeš, L. and Pšencík, I., 1988. Complete seismic ray-tracing in three-dimensional structures. In: Doornbos, D.J. (Ed.), Seismological Algorithms: 89-168, Academic Press, New York.

Cormier, V.F. and Mellen, M.H.,1984. Application of asymptotic ray theory to vertical seismic profiling. In: Toksöz, M.N. and Stewart, R.R. (Eds.), Vertical Seismic Profiling, Advanced Concepts: 28-44. Geophysical Press, Amsterdam.

Klimeš, L., 1996. Accuracy of finite-differences in smooth media. Pure Appl. Geophys., 148: 39-76.

Klimeš, L., 2019. Comparison of ray-matrix and finite-difference methods in a simple 1-D velocity model. Studia Geophys. Geodet., 63: 247-256.

Klimeš, L., 2020. Effects of causal and noncausal attenuation in 2-D model UNCONFORMITY. Studia Geophys. Geodet., submitted.

Küpper, F.J., 1958. Theoretische Untersuchungen über die Mehrfachaufstellung von Geophonen (In German). Geophys. Prosp., 6: 194-256.

Müller, G., 1970. Exact ray theory and its application to the reflection of elastic waves from vertically inhomogeneous media. Geophys. J. Roy. Astron. Soc., 21: 261-284.

Musil, M., 1989. Computation of synthetic seismograms in 2-D and 3-D media using the Gaussian beam method. Studia Geophys. Geodet., 33: 213-229.

Zahradník, J., 1995. Simple elastic finite-difference scheme. Bull. Seismol. Soc. Am., 85: 1879-1887.

Zahradník, J. and Priolo, E., 1995. Heterogeneous formulations of elastodynamic equations and finite-difference schemes. Geophys. J. Internat., 120: 663-676.